Available online at www.sciencedirect.com
ScienceDirect
Journal of Organometallic Chemistry 692 (2007) 4327–4336
Journal of Organometallic Chemistry
www.elsevier.com/locate/jorganchem

Organo-aluminum, zinc and magnesium derivatives of the imidotris(amido)phosphate $Me_3SiNP(NH^tBu)_3$

Stuart D. Robertson, Tristram Chivers *, Jari Konu

Department of Chemistry, University of Calgary, Calgary, AB, Canada T2N 1N4

Received 12 June 2007; received in revised form 26 June 2007; accepted 27 June 2007
Available online 5 July 2007

Abstract

Reactions of $(^tBuHN)_3PNSiMe_3$ (**1**) with the alkyl-metal reagents dimethylzinc, trimethylaluminum and di-*n*-butylmagnesium yield the monodeprotonated complexes $[MeZn\{(N^tBu)(NSiMe_3)P(NH^tBu)_2\}]$ (**2**), $[Me_2Al\{(N^tBu)(NSiMe_3)P(NH^tBu)_2\}]$ (**3**) and $[Mg\{(N^tBu)(NSiMe_3)P(NH^tBu)_2\}_2]$ (**4**), respectively. Attempts to further deprotonate complex **2** with *n*-butyllithium or di-*n*-butylmagnesium result in nucleophilic displacement of the methylzinc fragment by lithium or magnesium. The two remaining amino protons of **3** are removed by reaction with di-*n*-butylmagnesium to give a heterobimetallic complex in which the coordination sphere of magnesium is completed by two molecules of THF (**5** · 2THF) or one molecule of TMEDA (**5** · TMEDA). Reaction of complex **3** with 1 equiv. of *n*-butyllithium followed by treatment of the product with di-*n*-butylmagnesium yields the complex $\{Me_2Al[(N^tBu)(NSiMe_3)P(N^tBu)_2]MgBu\}$ Li · 4THF (**6** · 4THF), the first example of a triply deprotonated complex of **1** containing three different metals. Reaction of complex **5** with iodine results in cleavage of an Al–Me group to give $\{MeIAl[(N^tBu)(NSiMe_3)P(N^tBu)_2Mg]\}$ (**7**). Complexes **5** · 2THF, **5** · TMEDA, **6** · 4THF and **7** have been characterized in solution by multinuclear (^1H, ^{13}C, ^{31}P and ^7Li) NMR spectroscopy, while the solid-state structures of **2**, **4** and **5** · 2THF have been determined by X-ray crystallography.

Keywords: Aluminum; Magnesium; Zinc; Imidophosphates; Structures; X-ray diffraction

1. Introduction

The synthesis of imido analogues of simple oxoanions such as carbonate, silicate and phosphate is an area of current interest in main group chemistry [1]. Since the imido ($[NR]^{2-}$) and oxo ($[O]^{2-}$) ligands are formally isoelectronic [2], the replacement of the oxygen atoms by imido groups generates a new series of polyanions, whose physical and chemical properties are different from those of the isoelectronic oxoanions owing to the influence of the R group on nitrogen. Typically the presence of these organic substituents leads to more soluble species with solid-state structures that are less associated than their oxo counterparts.

The first example of a tetraimido analogue of the orthophosphate anion, $[PO_4]^{3-}$, was obtained in low yield as the solvent-separated ion pair $[(THF)_4Li][(THF)_2Li(\mu\text{-}Nnaph)_2P(\mu\text{-}Nnaph)_2Li(THF)_2]$ by Russell and coworkers in 1997 [3] from a curious redox reaction between P_2I_4 and 1-aminonaphthalene in the presence of 4 equiv. of *n*-butyllithium. In an alternative approach to tetraimidophosphates we have shown that $(^tBuNH)_3PNSiMe_3$ (**1**) [4] can be sequentially deprotonated with *n*-butyllithium to give $Li[P(N^tBu)(NH^tBu)_2(NSiMe_3)]$ (**1Li**) [5], $Li_2[P(N^tBu)_2(NH^tBu)(NSiMe_3)]$ (**1Li$_2$**) [5] and $Li_3[P(N^tBu)_3(NSiMe_3)]$ (**1Li$_3$**) [4]. The anions in these complexes can be considered analogues of dihydrogen phosphate $[H_2PO_4]^-$, hydrogen phosphate $[HPO_4]^{2-}$ and orthophosphate $[PO_4]^{3-}$, respectively. The use of a similar strategy generated the trilithium derivative of the tetraanilido species $[P(NPh)_4]^{3-}$ from the phosphonium salt $[P(NHPh)_4]Cl$ and 4 equiv. of *n*-butyllithium, which was isolated as an LiCl adduct [6]. A fascinating feature of the reactivity of the tri-lithiated derivative (**1Li$_3$**) is its propensity to

* Corresponding author. Tel.: +1 403 220 5741; fax: +1 403 289 9488.
E-mail address: chivers@ucalgary.ca (T. Chivers).

0022-328X/$ - see front matter © 2007 Elsevier B.V. All rights reserved.
doi:10.1016/j.jorganchem.2007.06.064

undergo oxidation to form a stable, blue paramagnetic species which, in the solid state, exhibits a distorted cubic structure comprised of the dilithium derivative of the radical dianion $[P(N^tBu)_3(NSiMe_3)]^{2-\cdot}$ and a molecule of lithium iodide [7,8]. In THF solution, solvation of the Li^+ ions results in rupture of the cubic structure to generate spirocyclic complexes that incorporate this radical dianion [9,10].

Subsequent investigations of the deprotonation of $(^tBuNH)_3PNSiMe_3$ with alkyl-zinc, aluminum or magnesium reagents revealed that only mono-deprotonation was possible. The similar zinc (**2**) and aluminum (**3**) complexes were prepared by the alkane elimination reactions of **1** with dimethylzinc [11] or trimethylaluminum [12], respectively, as shown in Scheme 1. The coordination mode of the monoanionic ligand $[P(N^tBu)(NH^tBu)_2(NSiMe_3)]^-$ in **2** and **3** was deduced on the basis of solution NMR data, but the solid-state structures were not reported [11,12]. The reaction of **1** with di-*n*-butylmagnesium resulted in mono-deprotonation of 2 equiv. of **1**, yielding a magnesium complex that was assigned the spirocyclic structure (**4**) (Scheme 1) on the basis of solution NMR data [12]. Significantly, the coordination mode proposed for $[P(N^tBu)(NH^tBu)_2(NSiMe_3)]^-$ in **4** was different from that suggested for the zinc and aluminum complexes **2** and **3**, respectively [12].

The susceptibility of complexes **3** and **4** to further deprotonation by *n*-butyllithium to yield heterometallic complexes was subsequently examined. While no evidence for lithiation of **2** with *n*-butyllithium exists, the two remaining amino protons of the aluminum complex **3** were sequentially removed with 1 or 2 equiv. of *n*-butyllithium to yield a mono (**3Li**) and di-lithiated species (**3Li$_2$**), respectively, in which the ligand coordination mode was established by X-ray structural determinations (Scheme 2) [12]. The one-electron oxidation of **3Li$_2$** with iodine produces the persistent, neutral radical $[Me_2Al(\mu\text{-}N^tBu)(\mu\text{-}NSiMe_3)P(\mu\text{-}N^tBu)_2Li(THF)_2]$ identified in solution by EPR spectroscopy [12].

The objectives of the current work were (a) to establish whether the $[P(N^tBu)(NH^tBu)_2(NSiMe_3)]^-$ ligand adopts different bonding modes towards electropositive metals by determining the solid-state structures of **2**, **3** and **4**

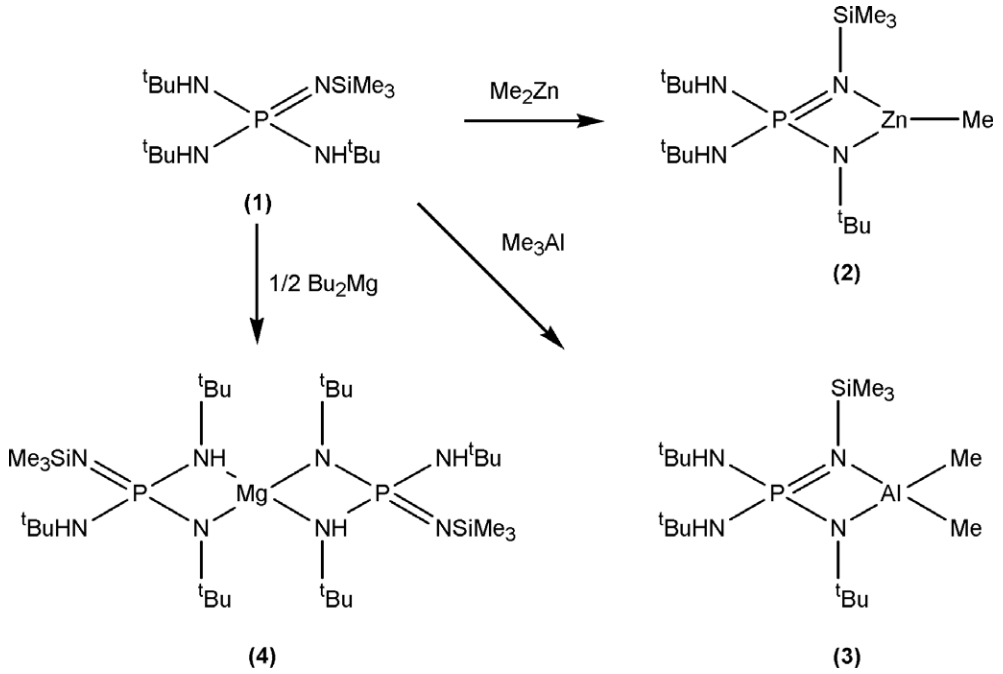

Scheme 1.

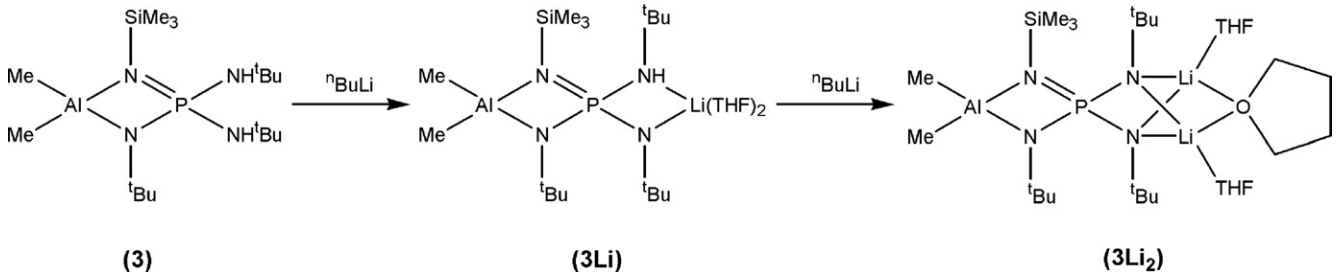

Scheme 2.

and (b) to extend the range of known heterometallic complexes of $(^tBuHN)_3P{=}NSiMe_3$ through investigations of the reactions of **2** and **3** with alkyl-metal reagents. Such complexes are expected to serve as precursors to persistent or stable radicals by analogy with the paramagnetic neutral species $[Me_2Al(\mu\text{-}N^tBu)(\mu\text{-}NSiMe_3)P(\mu\text{-}N^tBu)_2Li(THF)_2]$.

2. Experimental

2.1. General considerations

All experiments were carried out under an argon atmosphere using standard Schlenk techniques. Toluene, *n*-hexane and tetrahydrofuran (THF) were dried over Na/benzophenone, distilled and stored over molecular sieves prior to use. Dimethylzinc (2.0 M solution in toluene), di-*n*-butylmagnesium (1.0 M solution in heptanes), trimethylaluminum (2.0 M solution in hexanes) and *n*-butyllithium (2.5 M solution in hexanes) were used as received from Aldrich. $(^tBuHN)_3PNSiMe_3$ [4], $[MeZn\{(N^tBu)(NSiMe_3)\text{-}P(NH^tBu)_2\}]$ [11], $[Me_2Al\{(N^tBu)(NSiMe_3)P(NH^tBu)_2\}]$ [12] $[Me_2Al\{(N^tBu)(NSiMe_3)P(N^tBu)(NH^tBu)\}Li(THF)_2]$ [12] and $[Mg\{(N^tBu)(NSiMe_3)P(NH^tBu)_2\}_2]$ [12] were prepared as described previously. NMR data (^1H and ^{31}P) of complexes **2**–**4** are included here for comparison with new compounds.

^1H, ^{13}C and ^{31}P NMR spectra were collected on a Bruker DMX-300 spectrometer with chemical shifts reported relative to Me_4Si in $CDCl_3$ (^1H and ^{13}C) and 85% H_3PO_4 in D_2O (^{31}P). All spectra were collected at 22 °C. Elemental analyses were provided by the Analytical Services Laboratory, Department of Chemistry, University of Calgary.

2.2. Spectroscopic data of $[MeZn\{(N^tBu)(NSiMe_3)P(NH^tBu)_2\}]$ (2)

^1H NMR (C_6D_6, δ): 1.78 (br, 2H, NH), 1.27 (s, 9H, N^{t}Bu), 1.23 (s, 18H, NH^{t}Bu), 0.37 (s, 9H, $SiMe_3$), −0.03 (s, 3H, ZnMe). $^{31}P\{^1H\}$ NMR (C_6D_6, δ): 9.6 (s).

2.3. Reaction of 2 with 1 equiv. of n-butyllithium

A solution of *n*-butyllithium (0.30 mL, 2.5 M, 0.750 mmol) in hexanes was added to a solution of **2** (0.311 g, 0.751 mmol) in *n*-hexane (20 mL) at 22 °C. After 4 h, stirring was ceased to allow the precipitated solid to settle and the solvent was decanted. The remaining solid was dried *in vacuo* to leave a white powder (0.181 g, 57%) identified as **1Li**. ^1H NMR (C_6D_6, δ): 1.93 (br, 2H, NH), 1.41 (s, 9H, N^{t}Bu), 1.37 (s, 18H, NH^{t}Bu), 0.48 (s, 9H, $SiMe_3$). $^{31}P\{^1H\}$ NMR (C_6D_6, δ): −0.8 (s). Lit. values: ^1H NMR (C_6D_6, δ): 1.90, 1.38, 1.35, 0.46. $^{31}P\{^1H\}$ NMR (C_6D_6, δ): −0.80 [5].

2.4. Reaction of 2 with 2 equiv. of n-butyllithium

A solution of *n*-butyllithium (0.60 mL, 2.5 M, 1.50 mmol) in hexanes was added to a solution of **2** (0.311 g, 0.751 mmol) in *n*-hexane (20 mL) at 22 °C. After 4 h, stirring was ceased to allow the precipitated solid to settle and the solvent was decanted. The remaining solid was dried *in vacuo* to leave a white powder (0.254 g, 80%) identified as $\mathbf{1Li}_2$. ^1H NMR (THF-d_8, δ): 1.54 (br, 1H, NH), 1.31 (s, 9H, NH^{t}Bu), 1.23 (s, 18H, N^{t}Bu), −0.01 (s, 9 H, $SiMe_3$). $^{31}P\{^1H\}$ NMR (C_6D_6, δ): 0.18 (s). Lit. values: ^1H NMR (THF-d_8, δ): 1.55, 1.31, 1.23, −0.01. $^{31}P\{^1H\}$ NMR (C_6D_6, δ): 0.16. [5].

2.5. Reaction of 2 with 0.5 equiv. of di-n-butylmagnesium

A solution of di-*n*-butylmagnesium (0.50 mL, 1.0 M, 0.50 mmol) in heptanes was added to a solution of **2** (0.414 g, 1.00 mmol) in *n*-hexane (20 mL) at 22 °C. After stirring for 16 h, the solvent was removed *in vacuo* to leave a pale yellow solid (0.291 g, 68%) identified as **4**. ^1H NMR (C_6D_6, δ): 1.90 (br, 2H, NH), 1.83 (br, 2H, NH), 1.50 (s, 9H, N^{t}Bu), 1.40 (s, 9H, NH^{t}Bu), 1.33 (s, 9H, NH^{t}Bu), 0.51 (s, 9H, $SiMe_3$). ^{31}P NMR (C_6D_6, δ): 6.7 (s) (cf. NMR data reported for **4** below).

2.6. Spectroscopic data of $[Me_2Al\{(N^tBu)(NSiMe_3)\text{-}P(NH^tBu)_2\}]$ (3)

^1H NMR (C_6D_6, δ): 1.84 (br, 2H, NH), 1.30 (s, 9H, N^{t}Bu), 1.17 (s, 18H, NH^{t}Bu), 0.36 (s, 9H, $SiMe_3$), −0.21 (s, 6H, $AlMe_2$). $^{31}P\{^1H\}$ NMR (C_6D_6, δ): 5.4 (s).

2.7. Spectroscopic data of $[Mg\{(N^tBu)(NSiMe_3)\text{-}P(NH^tBu)_2\}_2]$ (4)

^1H NMR (C_6D_6, δ): 1.89 (br, 2H, NH), 1.84 (br, 2H, NH) 1.49 (s, 9H, N^{t}Bu), 1.40 (s, 9H, NH^{t}Bu), 1.33 (s, 9H, NH^{t}Bu), 0.51 (s, 9H, $SiMe_3$). $^{31}P\{^1H\}$ NMR (C_6D_6, δ): 6.7 (s).

2.8. Preparation of $\{Me_2Al[(N^tBu)(NSiMe_3)\text{-}P(N^tBu)_2]Mg\}\cdot 2THF$ ($\mathbf{5}\cdot 2THF$)

A solution of di-*n*-butylmagnesium (1.0 mL 1.0 M, 1.0 mmol) in heptanes was added to a clear, colorless solution of **3** (0.390 g, 1.0 mmol) in *n*-hexane (20 mL) at 22 °C. After 4 h a white precipitate had formed. The solvent was removed *in vacuo* and THF (10 mL) was added. This reaction mixture was allowed to stir for 1 h before the solvent was removed *in vacuo*. The remaining white solid was recrystallized from a THF/*n*-hexane solution at −18 °C to give the $\mathbf{5}\cdot 2THF$ as a white powder (0.423 g, 76%). ^1H NMR ($CDCl_3$, δ): 4.12 (s, 8H, THF), 2.08 (s, 8H, THF) 1.29 (s, 9H, N^{t}Bu), 1.23 (s, 18H, $2\times$N^{t}Bu), 0.09 (s, 9H, $NSiMe_3$), −0.90 (s, 6H, Me_2Al). $^{13}C\{^1H\}$ NMR ($CDCl_3$ δ): 70.6 (s, THF), 50.2 (s, *C*Me$_3$), 36.1 (d, C*Me*$_3$, $^3J(^{13}C\text{–}^{31}P) = 8.4$ Hz), 33.6 (d, C*Me*$_3$, $^3J(^{13}C\text{–}^{31}P) = 6.9$ Hz), 25.6 (s, THF), 4.1 (d, Si*Me*$_3$, $^3J(^{13}C\text{–}^{31}P) = 2.7$ Hz), −5.8 (s, Al*Me*$_2$). $^{31}P\{^1H\}$ NMR ($CDCl_3$ δ): 14.6 (s). Anal. Calcd for $C_{25}H_{58}O_2PN_4SiAlMg$: C, 53.90; H, 10.49; N, 10.06. Found: C, 54.05; H, 10.32; N, 10.07.

2.9. Preparation of {$Me_2Al[(N^tBu)(NSiMe_3)$-$P(N^tBu)_2]Mg\}\cdot TMEDA$ ($\mathbf{5}\cdot TMEDA$)

A solution of di-*n*-butylmagnesium (1.0 mL 1.0 M, 1.0 mmol) in heptanes was added to a clear, colorless solution of **3** (0.390 g, 1.0 mmol) in *n*-hexane (20 mL) at 22 °C. After 4 h a white precipitate had formed. The solvent was removed *in vacuo* and toluene (25 mL) was added. TMEDA (1 mL) was added via syringe, precipitating an off white powder. This solvent was removed *in vacuo*. The remaining white solid was recrystallized from a THF/*n*-hexane solution at −18 °C to give $\mathbf{5}\cdot$TMEDA as an off-white powder (0.360 g, 68%). ^{1}H NMR ($CDCl_3$, δ): 2.79 (s, 4H, $Me_2NCH_2CH_2NMe_2$), 2.71 (s, 6H, $Me_2NCH_2CH_2NMe_2$), 2.66 (s, 6H, $Me_2NCH_2CH_2NMe_2$), 1.38 (s, 9H, N^{t}Bu), 1.33 (s, 18H, 2 × N^{t}Bu), 0.19 (s, 9H, $NSiMe_3$), −0.82 (s, 6H, Me_2Al). $^{13}C\{^1H\}$ NMR ($CDCl_3$ δ): 57.1 (s, $Me_2NCH_2CH_2NMe_2$), 56.7 (s, $Me_2NCH_2CH_2NMe_2$), 47.8 (s, $Me_2NCH_2CH_2NMe_2$), 47.6 (s, $Me_2NCH_2CH_2NMe_2$), 36.4 (d, CMe_3, $^3J(^{13}C–^{31}P) = 8.3$ Hz), 33.7 (d, CMe_3, $^3J(^{13}C–^{31}P) = 6.9$ Hz), 4.2 (d, $SiMe_3$, $^3J(^{13}C–^{31}P) = 3.0$ Hz), −5.4 (s, $AlMe_2$). $^{31}P\{^1H\}$ NMR ($CDCl_3$ δ): 17.4 (s). Although the recrystallized sample of $\mathbf{5}\cdot$TMEDA was spectroscopically pure, several attempts to obtain satisfactory CHN analyses were unsuccessful.

2.10. Preparation of {$Me_2Al[(N^tBu)(NSiMe_3)P(N^tBu)_2]$-$MgBu\}Li\cdot 4THF$ ($\mathbf{6}\cdot 4THF$)

A solution of di-*n*-butylmagnesium (0.50 mL 1.0 M, 0.50 mmol) in heptanes was added to a clear, colorless solution of **3Li** (0.198 g, 0.50 mmol) in THF (20 mL) at 22 °C. After stirring for 2 h, the solvent was removed *in vacuo* to leave a white solid (0.298 g, 78%). ^{1}H NMR (THF-d_8, δ): 1.62 (m, 2H, $MgCH_2CH_2CH_2CH_3$), 1.35 (s, 9H, N^{t}Bu), 1.29 (s, 18H, N^{t}Bu) 1.26 (m, 2H, $MgCH_2CH_2CH_2CH_3$), 0.86 (m, 3H, $MgCH_2CH_2CH_2CH_3$), 0.12 (s, 9H, $NSiMe_3$), −0.56 (m, 2H, $MgCH_2CH_2CH_2CH_3$), −0.94 (s, 6H, Me_2Al). ^{7}Li NMR (THF-d_8 δ): −0.64 (s). $^{13}C\{^1H\}$ NMR (THF-d_8 δ): 67.2 (s, THF), 49.6 (s, CMe_3), 35.3 (d, CMe_3, $^3J(^{13}C–^{31}P) = 9.0$ Hz), 33.8 (s, $MgCH_2CH_2CH_2CH_3$) 33.5 (d, CMe_3, $^3J(^{13}C-^{31}P) = 6.7$ Hz), 32.0 (s, $MgCH_2CH_2CH_2CH_3$), 25.3 (s, THF) 13.9 (s, $MgCH_2CH_2CH_2CH_3$), 13.6 (s, $MgCH_2CH_2CH_2CH_3$), 8.3 (s, $AlMe_2$), 3.9 (d, $SiMe_3$, $^3J(^{13}C–^{31}P) = 2.3$ Hz). $^{31}P\{^1H\}$ NMR (THF-d_8 δ): 12.5 (s). Anal. Calc. for $C_{37}H_{83}O_4PN_4SiAlMgLi$: C, 58.06; H, 10.93; N, 7.32. Found: C, 57.33; H, 10.31; N, 6.81.

2.11. Preparation of {$MeIAl[(N^tBu)(NSiMe_3)$-$P(N^tBu)_2Mg]\}$ (7)

A solution of iodine (0.100 g, 0.395 mmol) in THF (10 mL) was added via cannula to a clear, colorless solution of $\mathbf{5}\cdot$2THF (0.220 g, 0.395 mmol) in THF (20 mL) at 22 °C. The deep color of the iodine dissipated immediately upon addition. The solvent was removed *in vacuo* to leave the product as a sticky pale blue solid (0.174 g, 66%). ^{1}H NMR (THF-d_8, δ): 1.33 (s, 9H, N^{t}Bu), 1.30 (s, 9H, N^{t}Bu), 1.28 (s, 9H, N^{t}Bu), 0.16 (s, 9H, $NSiMe_3$), −0.60 (s, 3H, MeIAl). $^{31}P\{^1H\}$ NMR ($CDCl_3$ δ): 12.3 (s). Satisfactory CHN analyses could not be obtained as this compound decomposed slowly in solution.

2.12. Crystallographic details

Colorless crystals of **2**, **4** and $\mathbf{5}\cdot$2THF were coated with Paratone 8277 oil and mounted on a glass fiber. Diffraction data were collected on a Nonius KappaCCD diffractometer using monochromated Mo Kα radiation ($\lambda = 0.71073$ Å) at −100 °C. The data sets were corrected for Lorentz and polarization effects, and empirical absorption correction was applied to the net intensities. The structures were solved by direct methods using SHELXS-97 [13] and refined using SHELXL-97 [14]. After the full-matrix least-squares refinement of the non-hydrogen atoms with anisotropic thermal parameters, the hydrogen atoms were placed in calculated positions [C–H = 0.98 Å for $C(CH_3)_3$ and 0.84 Å for amino hydrogens]. The isotropic thermal parameters of the hydrogen atoms were fixed at 1.2 times that of the corresponding nitrogen for amino hydrogens, and 1.5 times for $C(CH_3)_3$. In the final refinement the hydrogen atoms were riding with the carbon or nitrogen atom to which they were bonded.

Table 1
Crystallographic data for [MeZn{(N^{t}Bu)(NSiMe$_3$)P(NH^{t}Bu)$_2$}] (**2**), [Mg{(N^{t}Bu)- (NSiMe$_3$)P(NH^{t}Bu)$_2$}$_2$] (**4**) and {Me$_2$Al[(N^{t}Bu)(NSiMe$_3$)-P(N^{t}Bu)$_2$]Mg} ($\mathbf{5}\cdot$2THF)

	2	**4**	**5** · 2THF
Empirical formula	$C_{16}H_{41}N_4PSiZn$	$C_{38}H_{92}MgN_8O_2P_2Si_2$	$C_{25}H_{58}AlMgN_4O_2PSi$
fw	413.96	835.63	557.10
Crystal system	Orthorhombic	Orthorhombic	Orthorhombic
Space group	*Pbca*	*Aba*2	*Pca*2$_1$
a (Å)	16.624(3)	21.659(4)	20.263(4)
b (Å)	9.4389(19)	14.904(3)	9.992(2)
c (Å)	30.015(6)	15.786(3)	33.823(7)
α (°)	90	90	90
β (°)	90	90	90
γ (°)	90	90	90
V (Å^3)	4709.8(16)	5095.8(18)	6848(2)
Z	8	4	8
T (K)	173(2)	173(2)	173(2)
λ (Å)	0.71073	0.71073	0.71073
d_{calc} (g cm^{-3})	1.168	1.089	1.081
μ (mm^{-1})	1.167	0.182	0.185
θ Range (°)	3.27–25.03	3.39–25.02	3.39–25.03
Reflections collected	7777	4338	11,501
Unique reflections	4139	4336	11,501
R_{int}	0.0289		
F(000)	1792	1848	2448
R_1 [$I > 2\sigma(I)$][a]	0.0352	0.0404	0.0768
wR_2 (all data)[b]	0.0937	0.1066	0.1946
GOF of F^2	1.023	1.056	1.051

[a] $R_1 = \sum\|F_o| - |F_c\|/\sum|F_o|$.
[b] $wR_2 = [\sum w(F_o^2 - F_c^2)^2/\sum wF_o^4]^{1/2}$.

The structure of **4** shows two independent molecules in which the $NSiMe_3$ and adjacent N^tBu units exhibit disorder. Upon refinement, the disorder was resolved in terms of the silicon and α-carbon atoms of these groups being statistically distributed over the two atomic sites. The two atoms were not constrained to locate in the same position, but the anisotropic thermal parameters were restricted to be equal in the final refinement. The site occupation factors were approximately 60/40 in both molecules. The corresponding methyl groups, however, could not be refined as disordered. Crystallographic data are summarized in Table 1.

3. Results and discussion

3.1. Spectroscopic and structural characterization of $[MeZn\{(N^tBu)(NSiMe_3)P(NH^tBu)_2\}]$ (2)

Complex **2** was prepared by the literature procedure (Scheme 1) [11] and obtained as a white solid after recrystallization from THF/*n*-hexane. The ^1H NMR spectrum of **2** in C_6D_6 showed the expected broad signal of the amino protons at 1.78 ppm, a singlet at 0.37 ppm and a singlet at −0.03 ppm representing the trimethylsilyl and methylzinc fragments, respectively. The resonances for the two different *tert*-butyl environments appeared at 1.27 ppm (bridging N^tBu) and 1.23 ppm (terminal ^{t}BuNH groups) with relative intensities 1:2.

X-ray quality crystals of **2** were obtained from THF/*n*-hexane at 23 °C. The X-ray analysis revealed that **2** exists as a monomer (Fig. 1). The analogous complex $[MeZn(\mu\text{-}S)(\mu\text{-}N^tBu)P(NH^tBu)_2]_2$ forms a dimer with a ladder structure and a central Zn_2S_2 ring in the solid state [11]. Presumably, the presence of the bulky trimethylsilyl group on the imido nitrogen prohibits dimerization in the case of **2**. Selected bond lengths and bond angles are given in Table 2.

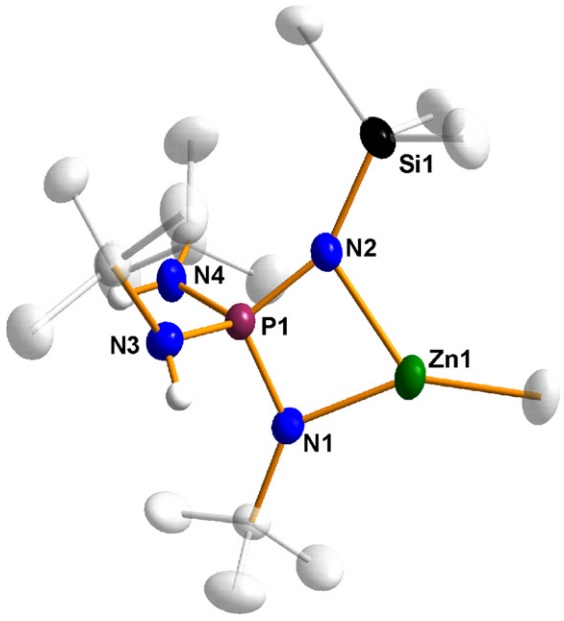

Fig. 1. Thermal ellipsoid plot of **2** (50% probability). Carbon-bound hydrogen atoms have been omitted for clarity.

Table 2
Selected bond lengths (Å) and bond angles (°) for **2**

Bond lengths (Å)			
Zn(1)–N(1)	1.944(2)	P(1)–N(2)	1.585(2)
Zn(1)–N(2)	2.102(2)	P(1)–N(3)	1.655(2)
Zn(1)–C(1)	1.939(3)	P(1)–N(4)	1.673(2)
P(1)–N(1)	1.618(2)	N(2)–Si(1)	1.699(2)
Bond and torsion angles (°)			
N(1)–Zn(1)–N(2)	74.8(1)	P(1)–N(1)–Zn(1)	94.7(1)
C(1)–Zn(1)–N(1)	151.7(1)	P(1)–N(1)–C(10)	131.8(2)
C(1)–Zn(1)–N(2)	133.5(1)	Zn(1)–N(1)–C(10)	133.3(2)
N(1)–P(1)–N(2)	100.4(1)	P(1)–N(2)–Zn(1)	89.8(1)
N(1)–P(1)–N(3)	117.6(1)	P(1)–N(2)–Si(1)	152.2(1)
N(1)–P(1)–N(4)	106.9(1)	Zn(1)–N(2)–Si(1)	117.8(1)
N(2)–P(1)–N(3)	113.1(1)	N(1)–P(1)–N(2)–Zn(1)	−4.3(1)
N(2)–P(1)–N(4)	120.4(1)	N(1)–Zn(1)–N(2)–P(1)	3.64(9)
N(3)–P(1)–N(4)	99.4(1)		

The solid-state structure of **2** confirms the structure previously proposed on the basis of NMR data [11]; the N^tBu and $NSiMe_3$ groups are chelated to the zinc centre. As expected, the mean P–N bond lengths involving the terminal NH^tBu groups (1.664(2) Å) are significantly longer than the bridging P–N(^{t}Bu) bond (1.618(2) Å). This difference in the P–N bond lengths is consistent with the values reported for other complexes in which a PN_4 ligand involving both amido and imido groups is N-bound to a metal centre [15–17]. This bridging P–N^tBu bond is also substantially shorter than the mean P–N(H)^{t}Bu bond length in (**1**) (1.667(1) Å) [4]. Meanwhile, the P–N($SiMe_3$) bond is lengthened by ca. 0.07 Å with respect to that in **1** as a consequence of the donation of electron density towards the zinc cation, which is also reflected in the modest elongation of the N–Si bond from 1.667(2) Å in **1** to 1.699(2) Å in complex **2**. The Zn–N^tBu bond length of 1.944(2) Å is substantially shorter than the bond between the positive zinc centre and the $NSiMe_3$ group (2.102(2) Å), suggesting that the negative charge resides primarily on the N^tBu nitrogen atom. These metal-nitrogen bonds are similar in length to those observed in other PN_2Zn ring-containing complexes [17–19]. The disparity of ca. 0.16 Å in the two N–Zn bond lengths gives rise to a highly distorted four-membered PN_2Zn ring in **2,** in contrast to the related complex containing a PN_2Zn ring, ^{t}BuNH(S)P(μ–N^tBu)$_2$P(μ-N^tBu)(μ-N-*p*-tolyl)ZnEt, in which both the P–N and the Zn–N bonds are equal in length [17]. The four-membered ring is approximately planar, with the dihedral angles being less than 5°. The geometry around zinc is trigonal planar ($\Sigma < Zn = 360°$). As expected, chelation of the zinc atom gives rise to a distorted tetrahedral geometry at the phosphorus centre ($\angle$N–P–N = 100.4(1)–120.4 (1)°). The P–N–Si angle of 152.2(1)° is substantially larger than expected for a three-co-ordinate nitrogen atom, possibly as a result of the stereochemical influence of the two bulky N(H)^{t}Bu groups.

Crystals of the analogous aluminum complex **3** were obtained from a THF solution layered with *n*-hexane. An

X-ray structural determination confirmed the previously assigned coordination mode of the $[P(N^tBu)(NH^tBu)_2(NSiMe_3)]^-$ligand based on NMR data (Scheme 1) [12]. However, twinning problems resulted in a poorly refined structure. Consequently, discussion of the details of bond lengths and bond angles is not warranted.

3.2. Spectroscopic and structural characterization of $[Mg\{(N^tBu)(NSiMe_3)P(NH^tBu)_2\}_2]$ (4)

The structure proposed for complex **4** (Scheme 1) was based on the observation of three equally intense resonances for the N^{t}Bu groups in the ^{1}H NMR spectrum [12]. An alternative structure, in which the $[P(N^tBu)(NH^tBu)_2(NSiMe_3)]^-$ ligand is coordinated to magnesium in the same manner as it is in **2** and **3**, is depicted in Fig. 2. This spirocyclic structure, with S_4 molecular symmetry, would also give rise to the three N^{t}Bu resonances. An X-ray structural determination of **4** was carried out in order to distinguish between these two alternatives.

X-ray quality crystals of **4** were obtained from layered solutions of THF/*n*-hexane at 23 °C. As illustrated in Fig. 3, the two $[P(N^tBu)(NH^tBu)_2(NSiMe_3)]^-$anions in **4** are chelated to the metal centre in the same way that this ligand is coordinated to zinc and aluminum in **2** and **3**, respectively. Selected bond lengths and bond angles of **4** are given in Table 3.

Like complex **2**, the mean P–N bond lengths involving the terminal NH^{t}Bu groups (1.673(2) Å) in **4** are significantly longer than the bridging P–N(^{t}Bu) bond (1.607(2) Å). The P–N(SiMe$_3$) bond is ca. 0.08 Å longer than that

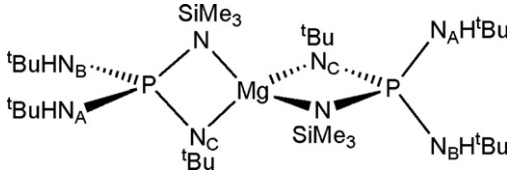

Fig. 2. Alternative structure of complex **4**.

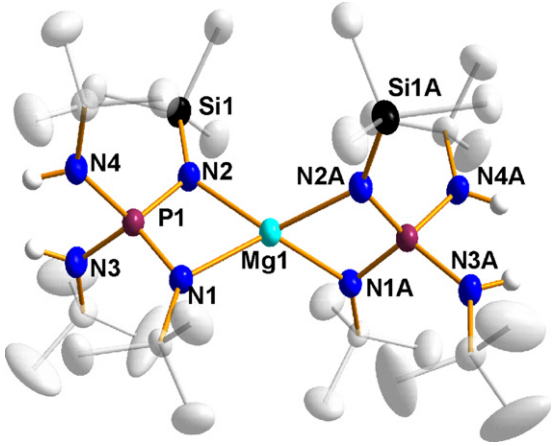

Fig. 3. Thermal ellipsoid plot of **4** (50% probability). Carbon-bound hydrogen atoms and the solvent molecule (THF) have been omitted for clarity.

Table 3
Selected bond lengths (Å) and bond angles (°) for **4**[a]

Bond lengths (Å)			
Mg(1)–N(1)	2.059(2)	P(1)–N(3)	1.677(2)
Mg(1)–N(2)	2.114(2)	P(1)–N(4)	1.668(2)
P(1)–N(1)	1.607(2)	N(2)–Si(1)	1.706(2)
P(1)–N(2)	1.601(2)		
Bond and torsion angles (°)			
N(1)–Mg(1)–N(2)	72.4 (1)	N(3)–P(1)–N(4)	95.4(1)
N(1)–Mg(1)–N(1)A	129.4(1)	P(1)–N(1)–Mg(1)	94.5(1)
N(1)–Mg(1)–N(2)A	132.1(1)	P(1)–N(1)–C(10)	129.0(2)
N(2)–Mg(1)–N(1)A	132.08(9)	Mg(1)–N(1)–C(10)	136.3(2)
N(2)–Mg(1)–N(2)A	129.0(1)	P(1)–N(2)–Mg(1)	92.6(1)
N(1)–P(1)–N(2)	100.4(1)	P(1)–N(2)–Si(1)	129.5(1)
N(1)–P(1)–N(3)	115.8(1)	Mg(1)–N(2)–Si(1)	137.9(1)
N(1)–P(1)–N(4)	116.4(1)	N(1)–P(1)–N(2)–Mg(1)	−2.1(1)
N(2)–P(1)–N(3)	115.8(1)	N(1)–Mg(1)–N(2)–P(1)	1.72(9)
N(2)–P(1)–N(4)	114.1(1)		

[a] Symmetry transformations used to generate equivalent atoms: $1-x$, $-y$, z.

in **1** and the Si–N bond is elongated to 1.706(2) Å in **4** from 1.667(2) Å in **1**, consistent with donation of electron density from NSiMe$_3$ to magnesium. The Mg–N^{t}Bu bond (2.059(2) Å) is significantly shorter than the Mg–NSiMe$_3$ bond (2.114(2) Å), as a consequence of the cation–anion interaction between the metal centre and N(1). These Mg–N bond lengths are consistent with those reported previously for complexes containing a N–Mg–N fragment with one bond considered to be dative [20].

The dihedral angles of the four-membered MgN$_2$P ring [2.2(1)° and 1.7(1)°] show it to be planar. The N–Mg–N bond angle in **4** is 72.4(1)°, cf. ∠N–Zn–N = 74.8(1)° in **2**. The endocyclic N–P–N bond angle (100.4(1)°) is similar to that of **2**. The bond angles around N(2) are much closer to the expected values of 120° in complex **4** compared with those in complex **2**, as illustrated by the P–N–Si angle of 129.5(1)° in **4** (cf. 152.2(1)° in **2**). The narrower P–N–Si bond angle in **4** may be attributed to the observation that the stereochemical influence of the two terminal NH^{t}Bu groups is opposed by the steric effect of bridging N^{t}Bu and NSiMe$_3$ groups in **4,** cf. the Me group attached to Zn in **2**. This also has an influence on the M–N–Si angle, making it considerably larger than the corresponding angle in **2**. Meanwhile, the bond angles around N(1) in **4** are in the narrow range 114.1(1)–116.4(1)° resulting in a less distorted structure than **2**. Finally, the magnesium centre is in a highly distorted tetrahedral environment due to the tight bite angle of the imido(amido)phosphate ligand that renders the N–Mg–N angle within the ligand to be significantly smaller (72.4(1)°) than the corresponding angles between the two ligands (129.0(1)–132.1(1)°).

3.3. Metallation reactions of zinc complex 2

While the two amino protons in complex **3** can be sequentially removed with *n*-butyllithium (Scheme 2) [12], reactions involving the deprotonation of the zinc analogue **2** with alkyl-metal reagents have not been reported. Such

heterobimetallic complexes are of interest given the intriguing structural and radical chemistry demonstrated by **3Li** and **3Li**$_2$ [12].

Reaction of **2** with one or two equiv. of *n*-butyllithium in *n*-hexane, respectively, produces white powders in good yield. However, the ^{1}H NMR spectra of these products did not show the expected Zn–CH$_3$ resonance in the region between 0 and −1 ppm. The ^{31}P NMR spectra revealed that the products of these two reactions were the known complexes **1Li** and **1Li**$_2$, respectively. The monolithiated complex **1Li** is formed by nucleophilic displacement of the MeZn fragment by *n*-butyllithium (Scheme 3); the volatile by-product MeZn^{n}Bu is presumably removed with the solvent under vacuum.

When two equiv. of *n*-butyllithium are utilized, the first equivalent is believed to generate **1Li** as shown in Scheme 3, while the second equivalent then deprotonates **1Li** to give **1Li**$_2$ (lithiation of **1Li** with *n*-butyllithium is the currently accepted synthesis of **1Li**$_2$) [5]. Attempts to prepare zinc-containing analogues of **3Li** or **3Li**$_2$ by the reaction of **1Li** or **1Li**$_2$ with Me$_2$Zn were unsuccessful; unreacted **1Li** and **1Li**$_2$ were recovered from the reaction mixtures.

Deprotonation of complex **2** was also attempted using di-*n*-butylmagnesium and trimethylaluminum. The reaction of **2** with half an equivalent of di-*n*-butylmagnesium yielded the known magnesium complex **4**, identified by ^{1}H and ^{31}P NMR spectra. The formation of **4** is thought to involve nucleophilic displacement of the MeZn units in **2** by the organomagnesium reagent (Scheme 4). No reaction occurred between **2** and trimethylaluminum at room temperature in *n*-hexane.

3.4. Synthesis and X-ray structure of {Me$_2$Al[(N^{t}Bu)(NSiMe$_3$)P(N^{t}Bu)$_2$]Mg} (5)

In view of the facile lithiation of **3** with *n*-butyllithium to give **3Li** and **3Li**$_2$ (Scheme 2) [12], we turned our attention to the reaction of **3** with di-*n*-butylmagnesium. When this reaction is carried out in a 1:1 molar ratio in *n*-hexane, the new heterobimetallic complex {Me$_2$Al[(N^{t}Bu)(NSiMe$_3$)P(N^{t}Bu)$_2$]Mg} (**5**) is obtained in good yield via double deprotonation of **3** by di-*n*-butylmagnesium (Scheme 5). When this reaction is carried out in a 2:1 molar ratio only 1 equiv. of **3** is consumed and complex **5** is again formed; there is no NMR evidence for the formation of a ML$_2$ complex of the type represented by the magnesium complex **4**. Complex **5** is the first example of a heterobimetallic complex of a tetraimidophosphate trianion that does not contain lithium.

The complex **5** is initially prepared in *n*-hexane and obtained as a white powder in almost quantitative yield after removal of the solvent *in vacuo*. The solution NMR spectra of this powder (both ^{1}H and ^{31}P) show multiple peaks in a non-coordinating solvent such as toluene or chloroform, possibly owing to the presence of various oligomers in solution. However, well-resolved NMR spectra are obtained by using a coordinating solvent such as tetrahydrofuran. A solitary resonance at 14.6 ppm is found in

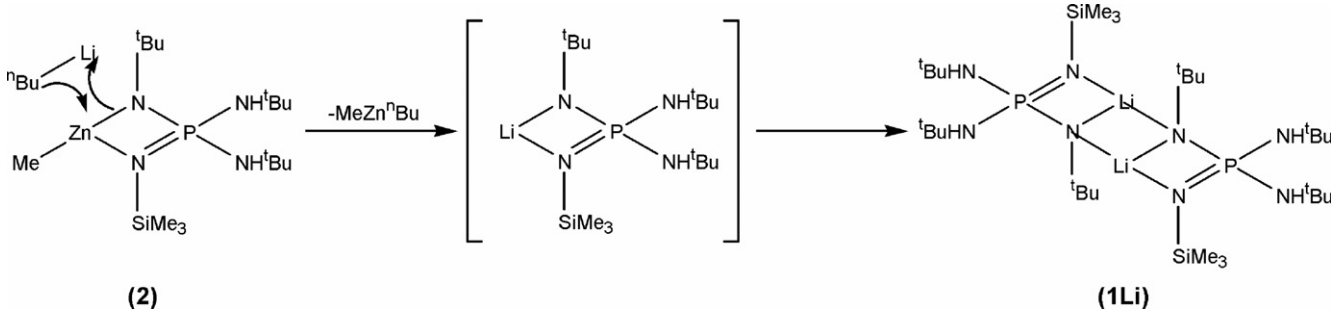

Scheme 3.

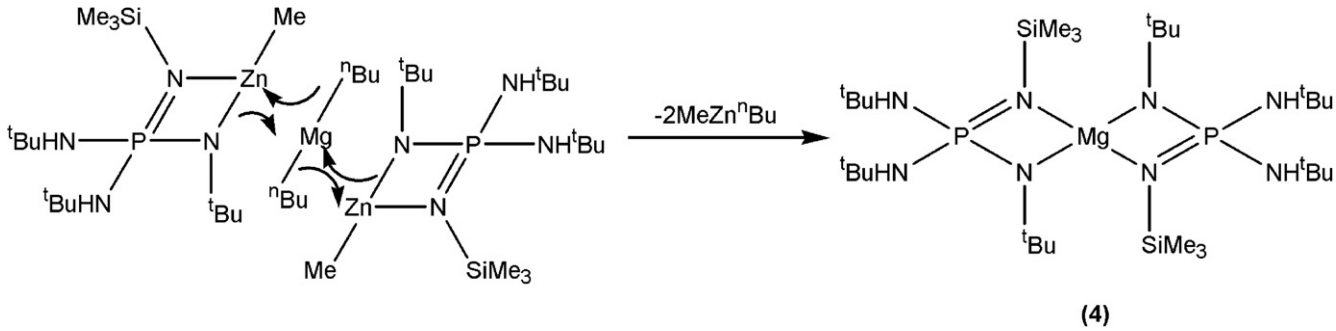

Scheme 4.

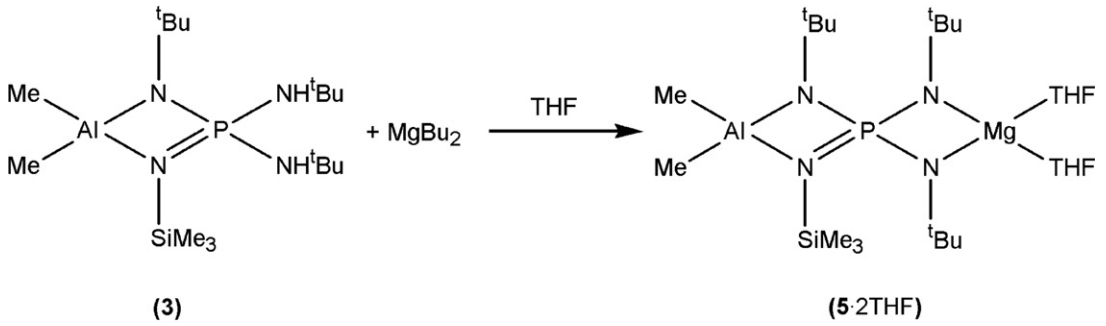

(3) (5·2THF)

Scheme 5.

the ^{31}P NMR spectrum while four singlets are observed in the ^{1}H NMR spectrum. The two methyl groups bonded to Al give a peak at −0.97 ppm, the trimethylsilyl group resonates at 0.07 ppm, while the two Mg–N^{t}Bu groups are at 1.26 ppm and the unique N^{t}Bu group is at 1.29 ppm. The relative intensities of these four resonances are in the expected 6:9:18:9 ratio. The simplification of the NMR spectra upon changing from a non-coordinating to a coordinating solvent suggests that coordination of solvent molecule(s) to the metal centre breaks up an associated structure. Therefore, the powder was recrystallized from a mixture of THF and *n*-hexane. NMR spectra of the resulting crystals were obtained in $CDCl_3$. The ^{31}P NMR spectrum exhibits a single peak at 14.6 ppm, while the ^{1}H NMR spectra showed only minor perturbations in chemical shifts (compared to the values observed in THF), as well as resonances at 2.08 and 4.12 ppm attributed to two coordinated THF molecules on the basis of the integrated relative intensities (Scheme 5).

Complex **5** can also be easily obtained as a *N*,*N*,*N*′,*N*′-tetramethylethylenediamine (TMEDA) solvate by addition of TMEDA to a stirred solution of the powdered product in toluene. The ^{31}P NMR spectrum of **5** · TMEDA exhibits a singlet at 17.4 ppm, while the ^{1}H NMR spectrum shows the Al–CH_3 group at −0.82 ppm, the trimethylsilyl group at 0.19 ppm, the equivalent N^{t}Bu groups at 1.33 ppm and the Al-bound N^{t}Bu group at 1.38 ppm. The resonances for the TMEDA protons are observed at 2.66, 2.71 and 2.79 ppm with relative intensities of 6:6:4.

The X-ray crystal structure of **5** · 2THF (Fig. 4) is consistent with NMR data, confirming that two molecules of THF are coordinated to magnesium. Selected bond lengths and angles are provided in Table 4 (values of only one of the two independent molecules in the crystal lattice are shown; bond parameters of the second molecule are identical).

This structure is shown to be spirocyclic, with two PN_2M rings sharing a common phosphorus atom. The two metal atoms are also four-coordinate, with the aluminum atom being capped by two methyl groups and the magnesium atom coordinated to two THF molecules via their oxygen atoms. The Al, P, and Mg atoms are all in distorted tetrahedral coordination spheres with endocyclic bond angles that are substantially smaller than the corresponding exocyclic bond angles for Al and Mg due to the constraints imposed by the four-membered AlN_2P and MgN_2P rings. The bond angles at the spirocyclic P centre are in the range 92.7(3)–118.6(3)°. The Mg–N bond lengths (1.978(5) Å and 2.007(5) Å), however, are significantly shorter (by *ca.* 0.09 Å) than those in **4**. In view of the disorder between N^{t}Bu and $NSiMe_3$ groups further discussion of structural parameters is not warranted. An X-ray structural determination confirmed the atomic connectivities in **5** · TMEDA illustrated in Fig. 5. The X-ray structure is consistent with the observed inequivalence of the two NMe_2 resonances of the TMEDA ligand. However, the data set was of poor quality and detailed discussion is not appropriate.

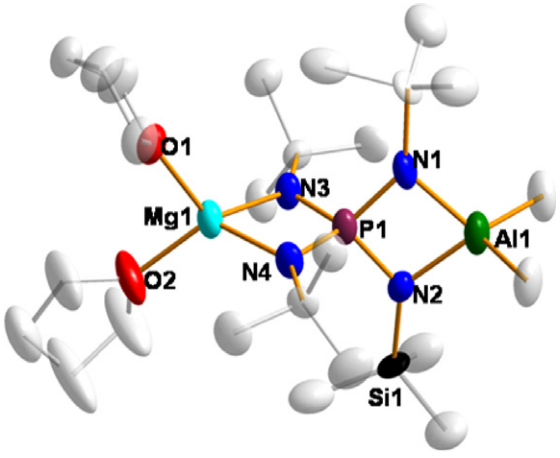

Fig. 4. Thermal ellipsoid plot of **5** · 2THF (50% probability). Hydrogen atoms have been omitted for clarity.

3.5. Synthesis of {$Me_2Al[(N^tBu)(NSiMe_3)P(N^tBu)_2]$-$MgBu$}$Li$ · 4THF (**6** · 4THF)

In light of the success in the synthesis of the bimetallic complex **5**, we considered the possibility of making a tetraimidophosphate complex containing three different metals. Again, the aluminum-containing complex (**3**) was considered a suitable starting point for such a complex owing to its established susceptibility to further metalla-

Table 4
Selected bond lengths (Å), bond and torsion angles (°) for **5** · 2THF

Bond lengths (Å)			
Al(1)–N(1)	1.883(6)	P(1)–N(4)	1.621(5)
Al(1)–N(2)	1.882(6)	N(2)–Si(1)	1.553(10)
Al(1)–C(1)	1.991(7)	Mg(1)–N(3)	1.978(5)
Al(1)–C(2)	1.985(7)	Mg(1)–N(4)	2.007(5)
P(1)–N(1)	1.653(6)	Mg(1)–O(1)	2.008(5)
P(1)–N(2)	1.665(6)	Mg(1)–O(2)	2.014(5)
P(1)–N(3)	1.651(5)		
Bond and torsion angles (°)			
N(1)–Al(1)–N(2)	79.2(3)	P(1)–N(1)–C(10)	136(2)
N(1)–Al(1)–C(1)	115.8(3)	Al(1)–N(2)–P(1)	93.8(3)
N(1)–Al(1)–C(2)	119.9(3)	Al(1)–N(2)–Si(1)	127.6(4)
C(1)–Al(1)–N(2)	116.0(4)	P(1)–N(2)–Si(1)	138.5(4)
C(1)–Al(1)–C(2)	108.0(4)	N(3)–Mg(1)–N(4)	75.6(2)
C(2)–Al(1)–N(2)	116.0(3)	O(1)–Mg(1)–O(2)	94.3(2)
N(1)–P(1)–N(2)	92.7(3)	N(3)–Mg(1)–O(1)	124.1(2)
N(1)–P(1)–N(3)	117.4(3)	N(3)–Mg(1)–O(2)	118.6(2)
N(1)–P(1)–N(4)	116.9(3)	N(4)–Mg(1)–O(1)	123.7(2)
N(2)–P(1)–N(3)	116.7(3)	N(4)–Mg(1)–O(2)	123.6(2)
N(2)–P(1)–N(4)	118.6(3)	N(1)–P(1)–N(2)–Al(1)	2.9(3)
N(3)–P(1)–N(4)	96.5(2)	N(1)–Al(1)–N(2)–P(1)	−2.6(3)
Al(1)–N(1)–P(1)	94.2(3)	N(3)–P(1)–N(4)–Mg(1)	4.8(2)
Al(1)–N(1)–C(10)	128(2)	N(3)–Mg(1)–N(4)–P(1)	−4.1(2)

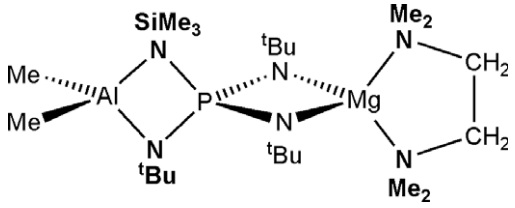

Fig. 5. Structure of complex **5** · TMEDA.

tion. To this end we investigated the deprotonation of **3Li** with di-*n*-butylmagnesium. This reaction proceeds well in a 1:1 molar ratio to yield the heterotrimetallic complex **6** as shown in Scheme 6.

The complex **6** is initially prepared in THF and the final product is obtained as a pale powder in good yield after removing the solvent *in vacuo*. The ^{1}H NMR spectrum in THF shows the three N^{t}Bu groups in a 1:2 integrated ratio, as expected for the spirocyclic anion depicted in Scheme 6. The Me_3Si and $AlMe_2$ groups also provide sharp singlets at 0.12 and −0.94 ppm, respectively. The Mg–$CH_2CH_2CH_2$-CH_3 group is represented by four multiplets of low intensity. As expected, the protons of the Mg–CH_2 group resonate at high field (−0.56 ppm). The ^{31}P NMR and ^{7}Li NMR spectra both display singlets at 12.5 ppm and −0.64 ppm, respectively.

The ^{1}H NMR spectrum of crystals of complex **6** in $CDCl_3$ also show the presence of coordinated THF. Two resonances at 3.86 and 1.91 ppm are present and integration of these peaks with respect to the *tert*-butyl and trimethylsilyl groups suggests that four molecules of THF are present in this complex. This, along with the fact that two of the ^{t}Bu groups are equivalent, allows us to conclude that this complex exists as an ion pair with the lithium cation solvated by four molecules of THF (Scheme 6). Compound **6**, to the best of our knowledge, is the first example of a complex of a tetraimidophosphate trianion containing three different metals.

3.6. Synthesis and NMR spectra of {MeIAl[(N^{t}Bu)-(NSiMe$_3$)P(N^{t}Bu)$_2$Mg]} (7)

We investigated the stoichiometric oxidation of **5** with iodine in an attempt to generate the corresponding radical cation with an iodide counter-anion. However, addition of 0.5 equiv. of I_2 to a colorless solution of **5** in THF results in a colorless solution with no indication of radical formation. The ^{31}P NMR displays two peaks of equal intensity at 12.3 and 14.6 ppm; the latter is attributed to unreacted **5**. When the reaction of **5** and I_2 is carried out in a 1:1 molar ratio, only the peak at 12.3 ppm is observed in the ^{31}P NMR spectrum of the isolated product. The ^{1}H NMR spectrum of this product shows three N^{t}Bu resonances of equal intensity. Furthermore, the integration of the spectrum indicated that only one methyl group is bound to aluminum, suggesting that the reagent I_2 has cleaved one of the Al–Me bonds in **5** to give {MeIAl[(N^{t}Bu)(NSiMe$_3$)P(N^{t}Bu)$_2$Mg]} (**7**) containing an Al–I bond (Scheme 7). Attempts to ascertain the structure of **7** through an X-ray structural

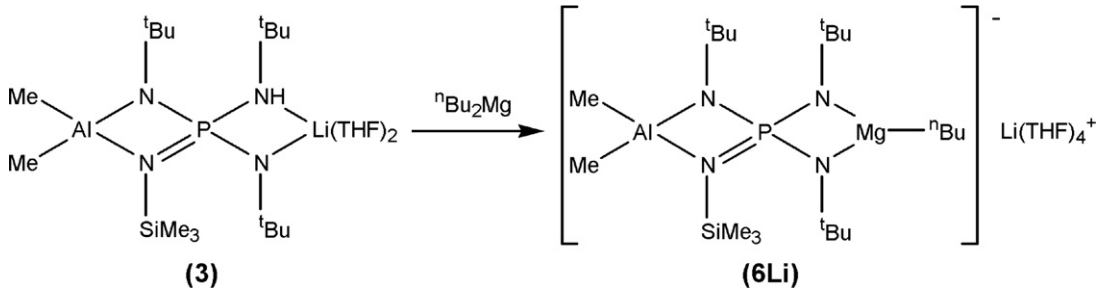

Scheme 6.

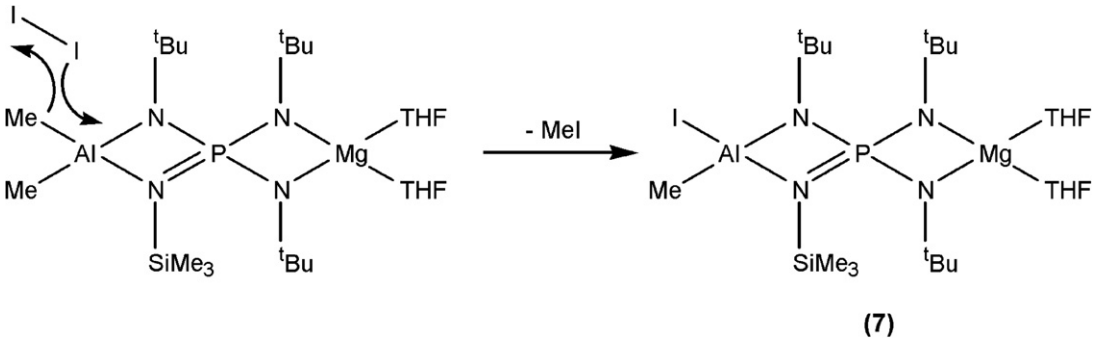

Scheme 7.

determination have not been successful owing to facile decomposition in solution.

4. Conclusions

Complexes of the chelating monoanionic ligand $[P(N^tBu)(NH^tBu)_2(NSiMe_3)]^-$ with methylzinc, dimethylaluminum or magnesium all involve coordination of the metal centre to the trimethylsilyl-bound nitrogen atom and an N^tBu group. Attempts to further metallate the zinc complex with *n*-butyllithium or di-*n*-butylmagnesium result in nucleophilic displacement of the methylzinc fragment by lithium to give known monometallic complexes. In a 1:1 molar ratio di-*n*-butylmagnesium doubly deprotonates the aluminum complex $[Me_2Al\{(N^tBu)(NSiMe_3)P(NH^tBu)_2\}]$ to yield the novel bimetallic complex $\{Me_2Al[(N^tBu)(NSiMe_3)P(N^tBu)_2]Mg\}$, which undergoes Al–methyl bond cleavage upon reaction with I_2. Di-*n*-butylmagnesium deprotonates the heterobimetallic complex $[Me_2Al\{(N^tBu)(NSiMe_3)P(NH^tBu)(N^tBu)\}Li]$ to yield the first tetraimidophosphate complex containing three different metals.

Acknowledgement

We thank the Natural Sciences and Engineering Research Council of Canada for funding.

Appendix A. Supplementary material

CCDC 650326, 650327 and 650328 contain the supplementary crystallographic data for **2**, **4** and **5** · 2THF. These data can be obtained free of charge via http://www.ccdc.cam.ac.uk/conts/retrieving.html, or from the Cambridge Crystallographic Data Centre, 12 Union Road, Cambridge CB2 1EZ, UK; fax: (+44) 1223-336-033; or e-mail: deposit@ccdc.cam.ac.uk. Supplementary data associated with this article can be found, in the online version, at doi:10.1016/j.jorganchem.2007.06.064.

References

[1] (a) For recent reviews see: J.K. Brask, T. Chivers, Angew. Chem., Int. Ed. Engl. 40 (2001) 3960;
(b) G.M. Aspinall, M.C. Copsey, A.P. Leedham, C.A. Russell, Coord. Chem. Rev. 227 (2002) 217.
[2] (a) I. Langmuir, J. Am. Chem. Soc. 41 (1919) 868;
(b) I. Langmuir, J. Am. Chem. Soc. 41 (1919) 1543.
[3] P.R. Raithby, C.A. Russell, A. Steiner, D.A. Wright, Angew. Chem., Int. Ed. Engl. 36 (1997) 649.
[4] A. Armstrong, T. Chivers, M. Krahn, M. Parvez, G. Schatte, Chem. Commun. (2002) 2332.
[5] A. Armstrong, T. Chivers, M. Parvez, G. Schatte, R.T. Boeré, Inorg. Chem. 43 (2004) 3453.
[6] J.F. Bickley, M.C. Copsey, J.C. Jeffery, A.P. Leedham, C.A. Russell, D. Stalke, A. Steiner, T. Stey, S. Zacchini, Dalton Trans. (2004) 989.
[7] A stable radical is defined as a species which is "inherently stable" as an isolated paramagnetic molecule, while a persistent radical is a species which has a "relatively long lifetime" under the conditions used to generate it, but which cannot be isolated or dimerizes to a diamagnetic species in the solid state. P. Power, Chem. Rev. 103 (2003) 789.
[8] A. Armstrong, T. Chivers, M. Parvez, R.T. Boeré, Angew. Chem., Int. Ed. Engl. 43 (2004) 502.
[9] A. Armstrong, T. Chivers, R.T. Boeré, in: M. Lattman, R.A. Kemp (Eds.), ACS Symp. Ser. 917 (2006) 66.
[10] A. Armstrong, T. Chivers, H.M. Tuononen, M. Parvez, R.T. Boeré, Inorg. Chem. 44 (2005) 7981.
[11] A.F. Armstrong, T. Chivers, M. Krahn, M. Parvez, Can. J. Chem. 83 (2005) 1768.
[12] A. Armstrong, T. Chivers, H.M. Tuononen, M. Parvez, Inorg. Chem. 44 (2005) 5778.
[13] G.M. Sheldrick, in: SHELXS-97, Program for Crystal Structure Determination, University of Göttingen, 1997.
[14] G.M. Sheldrick, in: SHELXL-97, Program for Crystal Structure Refinement, University of Göttingen, 1997.
[15] S.K. Pandey, A. Steiner, H.W. Roesky, D. Stalke, Inorg. Chem. 32 (1993) 5444.
[16] G.R. Lief, C.J. Carrow, L. Stahl, R.J. Staples, Organometallics 20 (2001) 1629.
[17] G.R. Lief, D.F. Moser, L. Stahl, R.J. Staples, J. Organomet. Chem. 689 (2004) 1110.
[18] G.T. Lawson, C. Jacob, A. Steiner, Eur. J. Inorg. Chem. (1999) 1881.
[19] U. Wirringa, H. Voelker, H.W. Roesky, Y. Shermolovich, L. Markovski, I. Uson, M. Noltemeyer, H.-G. Schmidt, J. Chem. Soc., Dalton Trans. (1995) 1951.
[20] T. Chivers, C. Fedorchuk, M. Parvez, Organometallics 24 (2005) 580.